HHS Public Access

Author manuscript

Ann Biomed Eng. Author manuscript; available in PMC 2015 July 01.

Published in final edited form as:

Ann Biomed Eng. 2013 April ; 41(4): 682–693. doi:10.1007/s10439-012-0702-5.

Endothelial dysfunction, arterial stiffening, and intima-media thickening in large arteries from HIV-1 transgenic mice

Laura Hansen[1], **Ivana Parker**[2], **Roy L. Sutliff**[3], **Manu O. Platt**[1,4], and **Rudolph L. Gleason Jr.**[1,2,4]

[1]The Wallace H. Coulter Department of Biomedical Engineering, Georgia Institute of Technology, Atlanta, GA

[2]The George W. Woodruff School of Mechanical Engineering, Georgia Institute of Technology, Atlanta, GA

[3]Department Medicine, Emory University/Atlanta VAMC, Atlanta, GA

[4]The Petit Institute for Bioengineering and Bioscience, Georgia Institute of Technology, Atlanta, GA

Abstract

HIV patients on highly active antiretroviral therapy (HAART) exhibit elevated incidence of cardiovascular disease, including a higher risk of myocardial infarction and prevalence of atherosclerotic lesions, as well as increases in markers of subclinical atherosclerosis including increased carotid artery intima-media thickness, increased arterial stiffness, and impaired flow-mediated dilation. Both HAART and HIV-infection are independent risk factors for atherosclerosis and myocardial infarction. Studies implicate the HIV proteins *tat*, *gp120*, *vpu*, and *nef* in early on-set atherosclerosis. The objective of this study was to quantify the role of expression of HIV-1 proteins on the vascular function, biomechanics, and geometry of common carotid arteries and aortas. This study employed NL4-3Δ *gag/pol* transgenic mice (HIV-Tg), which contain the genetic sequence for the HIV-1 proteins *env*, *tat*, *nef*, *rev*, *vif*, *vpr*, and *vpu* but lacks the *gag* and *pol* genes and reports that HIV-Tg mice have impaired aortic endothelial function, increased carotid intima-media thickness (c-IMT), and increased arterial stiffness. Further, HIV-Tg arteries show decreased elastin content, increased cathepsin K and cathepsin S activity, and increased mechanical residual stress. Thus, mice that express HIV proteins exhibit pre-clinical markers of atherosclerosis and these markers correlate with changes in markers of vascular remodeling. These findings are consistent with the hypothesis that HIV-proteins, independent of HAART treatment or HIV infection, could play a role in of the development of cardiovascular disease.

Keywords

HIV; atherosclerosis; vascular remodeling

Corresponding Author: Rudolph L. Gleason, Jr., Ph.D., The George W. Woodruff School of Mechanical Engineering, The Wallace H. Coulter Georgia Tech/Emory Department of Biomedical Engineering & The Petit Institute for Bioengineering and Bioscience, Georgia Institute of Technology, 315 Ferst Drive, IBB 2305, Atlanta, GA 30332, rudy.gleason@me.gatech.edu, (404) 385-7218 (phone), (404) 385-1397 (fax).

Introduction

Human immunodeficiency virus-1 (HIV-1) affects over 34 million people worldwide [1]. Due to the success of highly active antiretroviral therapy (HAART), HIV-1-infection has been transformed from a terminal diagnosis to a manageable chronic disease. HIV patients, however, have elevated incidence of dyslipidemia, lipodystrophy, insulin resistance, diabetes mellitus, and cardiovascular disease (CVD); the latter includes an elevated risk of myocardial infarction [2–4] and higher prevalence of atherosclerotic lesions [5–7], as well as increases in markers of subclinical atherosclerosis, including increased carotid artery intima-media thickness (c-IMT) [8–13], increased arterial stiffness [8, 14, 15], and impaired brachial artery flow-mediated dilation (FMD), an indicator of endothelial dysfunction [8, 9, 14, 16–20].

HAART drugs, particularly protease inhibitors [21–25], but also other drug classes [16, 26–28], are often implicated as a mediator of early on-set CVD. Data, however, also suggest that HIV, independent of HAART, can induce CVD [9, 13, 29]. Elevated c-IMT and impaired FMD have been observed in HIV positive/HAART naïve patients [9]. Exposure of endothelial cells *in vitro* to various HIV proteins decreases nitric oxide synthase and increases cell adhesion molecules, endothelial permeability, cell proliferation, cytokine signaling, apoptosis, and oxidative stress [30–32]; these mechanisms are all implicated in the development of atherosclerosis. However, there remains a need to investigate the effect of the viral proteins, independent of viral infection and HAART, on the vasculature in an *in vivo* model.

The purpose of this study was to determine the effects of HIV-1 proteins on endothelial function, intima-media thickness, and arterial stiffness in common carotid arteries and aortas in the NL4-3Δ *gag/pol* transgenic mouse (HIV-Tg). This is a non-infectious model with a 7.4 kb transgene that contains the genetic sequence for the HIV-1 proteins *env*, *tat*, *nef*, *rev*, *vif*, *vpr*, and *vpu*, but lacks the *gag* and *pol* genes and is thus unable to replicate [33]. Additional markers of vascular remodeling were also quantified; namely, collagen and elastin content, collagen fiber orientation, cathepsin activity, residual stress, and axial mechanical behavior of these arteries. Data indicate that common carotid arteries and aortas from HIV-Tg mice exhibited impaired endothelial function and elevated c-IMT and arterial stiffness. These changes were coincident with decreased elastin content, increased protease activity (cathepsins K and S), and increased residual stress in the artery wall, suggesting that vascular remodeling, due in part to synthesis, proteolytic degradation, and remodeling of key structural components of the arterial wall (e.g., elastin and collagen) occurs in parallel to impaired vascular function and plays a role in the observed changes the geometric properties (i.e., c-IMT) and biomechanical properties (e.g., arterial stiffness) of the artery wall. These findings are consistent with the hypothesis that HIV-1 proteins alone, independent of HAART treatment or HIV infection, could play a role in vascular remodeling associated with atherosclerosis.

Materials and Methods

HIV-Transgenic Mouse Model

Male hemizygous NL4-3Δ *gag/pol* transgenic and wild-type littermate (FVB/N) mice, 10–12 weeks old, were euthanized with CO_2 and the right and left common carotids arteries and the aorta were removed and cleaned free of loose perivascular tissue. Unlike the homozygous HIV-1 Tg mice, which are smaller at birth, have decreased food intake compared to wild-type mice, and usually die within 40 days postnatal, the hemizygous mice appear normal at birth but develop signs of disease as they age, specifically renal failure known as HIV-associated nephropathy [33]. All work was conducted under the regulation of Georgia Institute of Technology's and Atlanta VA Medical Center's Institutional Animal Care and Use Committees (IACUC).

Endothelial Function Testing

The contractile and relaxation properties of the aorta were analyzed as described previously [34, 35]. 5-mm long rings from excised aortas, with intact endothelium, were maintained in physiological saline solution (PSS, 118 mM NaCL, 4.73 nM KCl, 1.2 mG $MgSO_4$, 0.025 mM EDTA, 1.2 mM KH_2PO_4, 2.5 mM $CaCl_2$, 11 mM glucose, and 25 mM NaH_2CO_3, at a pH of 7.4 when bubbled in 95% O_2/5% CO_2 at 37 C) and mounted on wire hooks attached to a Harvard Apparatus Differential Capacitor Force Transducer for isometric contraction. The rings were contracted with 300 nM phenylephrine to 80–90% of maximum contraction. The relaxation response of the precontracted rings to actetylcholine (1nM–100μM) and sodium nitroprusside, a nitric oxide (NO) donor, (0.1nM–1μM), was determined and recorded as a function of concentration.

Biomechanical Measurements: Cylindrical Biaxial Testing, Arterial Stiffness, and Opening Angle

Cylindrical Biaxial Testing—Cylindrical biaxial biomechanical tests of arteries were performed as previously described [36]. Excised common carotid arteries and aortas were maintained in culture medium (Dulbecco's modified Eagles medium containing 4.5g/L glucose and sodium pyruvate without L-glutamine and phenol red, Invitrogen, Inc.). For the aorta, branches within the suprarenal region were ligated using 10-0 silk sutures, and 8-0 suture was used to mount the arteries on two glass cannulae on the custom mechanical testing device [36]. The vessel and cannulae were suspended in a bath on the device, which was filled with media containing sodium nitroprusside (SNP) to ensure that the arteries were fully dilated during the mechanical tests. Perfusion of the vessel through the two glass cannulae allowed for careful control of the luminal pressure. The mounting cannulae were attached to computer controlled actuators that allowed for precise control of the vessel length, and an force transducer connected to one cannula allowed for the measurement of the axial load imposed on the vessel during testing. Thus, this computer-controlled device had the capability of maintaining precise luminal pressure and axial length of the vessel, while recording the outer diameter and axial force during the testing. All mechanical testing was completed within 2 hours following vessel excision.

Following preconditioning, fixed length pressure-diameter tests and fixed pressure force-length tests were performed under quasistatic loading conditions [36]. For pressure-diameter tests, vessels were cyclically inflated from 0 to 160 mmHg at a series of fixed axial stretches of λ=1.3, 1.4, 1.5, 1.6, 1.7, 1.8, and 1.9 (λ is the loaded vessel length/unloaded vessel length), with three loading/unloading cycles for each axial stretch. During the force-length tests vessels were held at constant pressures of 0, 40, 60, 80, 100, and 120 mmHg and cyclically stretched until a maximum axial load of 1 gram (for common carotid arteries) or 3 grams (for the aorta) with three loading/unloading cycles at each pressure. Repeatable mechanical loading curves were achieved after preconditioning and three loading cycles, indicating that this protocol achieved adequate preconditioning and that the maximum loads (160 mmHg and 1 gram) did not induce mechanical damage.

Arterial Stiffness—The Peterson's modulus (E_p), a common measure of arterial stiffness, was calculated as the slope of the pressure-outer diameter curve ($\Delta P/\Delta D$) at a given pressure normalized to the outer diameter (D) at that pressure; namely, $E_p = \Delta P/(\Delta D/D)$.

Opening Angles—Opening angle measurements were taken to quantify the residual stress in the unloaded configuration [37]. A 14% gelatin mixture was injected into the vessel, and a 7 series of segments were cut and placed in phosphate buffered saline (PBS) [38]. A single radial cut was made in each segment and the open sectors were allowed to equilibrate for 30 minutes. A dissection microscope and camera were used to collect images of the cross-sections of the sectors and an image processing script in MatLab (MathWorks) was used to quantify the vessel wall thickness H, inner arc length L_i, and outer arc length L_o of the open sector. The opening angle was calculated as $\theta = (L_o - L_i)/H$. Note, that θ is the half of the central angle of the stress free sector; thus, the traditional opening angle is $180 - \theta$ [37].

Intima-Media Thickness Measurements

The vessel wall thickness was quantified by two methods: two-photon imaging of live arteries mounted on the biomechanical testing device was used to quantify the intima-media thickness and adventitia thickness and standard histology of fixed, sectioned, and stained vessels was used as an additional measure to quantify intima-media thickness.

Two-Photon Microscopy—The custom biomechanical testing device fits on a LSM 510 META inverted confocal microscope (Zeiss) to visualize collagen and elastin, using their autofluorescent properties, across the entire wall of live, unfixed mouse arteries [36]. Isolated vessels, maintained in PSS, were excited with a 800 nm two-photon laser and collagen was visualized by detecting its second harmonic generation around 400 nm, and elastin emissions were detected by setting the META filter to a 480–560 nm bandpass configuration [39]. Z-stacks were collected at a variety of loading conditions including at a pressure of 100 mmHg and the *in vivo* axial stretch (λ = 1.7). Orthogonal views of these z-stacks were then used to calculate the thickness of the adventitial layer (collagen images) and intima-media layer (elastin images) of the arteries.

Histology—Vessels were fixed in 10% buffered formalin under no external loading, immersed in 30% sucrose overnight, embedded in optimal cutting temperature (OCT)

medium, and frozen. The arteries were cut into 7 μm thick slices, mounted on slides, and stained with hematoxylin and eosin. The images were analyzed using ImageJ (NIH) to quantify the thickness of the arteries.

Collagen Fiber Organization Measurements

The two-photon microscopy images were also used to quantify the angular distribution of collagen fibers within the arterial wall. The angles of fibers in each slice of the z-stack were quantified using a fast Fourier series algorithm program in a MATLAB script as established previously. [40, 41] Briefly, the initial processing included a low-pass filter, conversion to binary, and windowing with a 2D Tukey window. A fast Fourier transform of the preprocessed image generated a power spectrum. A histogram of the frequency of intensities between −90 and 90 degrees with 4 degree bins was created from the spectrum. This process was repeated for each slice within the z-stack to generate a distribution of fibers across the wall for each vessel. The thickness and relative wall location were normalized and the corresponding distributions in each vessel were averaged to create a surface which represented the fiber angle distributions through the wall for both groups. The mean mid-wall distribution and weighted mean fiber angle for each group were also calculated and compared.

Collagen and Elastin Content Measurements

Right and left common carotid arteries from a single mouse or a single suprarenal aorta were dried in a vacuum oven at 37°C for 2 days. The dry weight of the vessels was recorded for normalizing to protein content. For collagen analysis, collagen was solublized by placing the vessel in 0.5 mL of 0.5 M acetic acid containing pepsin with a 1:3 ratio of enzyme to tissue weight. The tubes containing the vessels were placed in a 37°C water bath for 48 hours with occasional agitation. Sirius red dye solution (0.3 mg/mL direct 80 Sirius red in 0.5 M acetic acid) was added to each tube and the solution was incubated at room temperature for 30 min. The supernatant was removed following centrifuging, 0.1 M HCl was added, and the sample was centrifuged again. 0.5 M NaOH was added and the samples were votexed to release the dye. The collagen content was then determined by measuring the absorbance of each sample at a wavelength of 540 nm.

The elastin content was quantified using the Fastin Elastin Assay (Biocolor). Elastin from the dried arteries was solublized by boiling in 0.25 M oxalic acid for 5 hours. Elastin in the sample solutions was then precipitated using the manufacturer’s precipitating agent. After 10 minutes the samples were centrifuged, and the supernatant was removed. The Fastin dye solution was then added to the tubes and allowed to bind with the precipitated elastin for 90 minutes. The samples were centrifuged again, and the unbound dye in the supernatant was removed. A dye dissociating solution was added to release the dye from the walls of the tube. The absorbance at 513 nm of the resulting solution was used to quantify the elastin content of the arteries.

Cathepsin Expression and Activity Measurements

Gelatin zymography—Excised suprarenal aortas were stored on ice in PBS and placed in 50 ul of lysis buffer (20 nM Tris–HCl [pH 7.5], 5 mM ethyleneglycoltetraacetic acid

[EGTA], 150 mM NaCl, 20 mM β-glycerol phosphate, 10 mM NaF, 1 mM sodium orthovanadate, 1% Triton X-100, and 0.1% Tween 20) with 0.1 mM leupeptin freshly added to stabilize enzymes during electrophoresis. Aortas were homogenized using disposable sample grinders (GE Healthcare), and protein concentrations were obtained by the bisinchoninic acid (BCA) assay (Pierce). Cathepsin zymography was performed as described previously [42, 43]. Briefly, 5X non-reducing loading buffer (0.05% bromophenol blue, 10% SDS, 1.5 M Tris, 50% glycerol) was added to all samples prior to loading. Equal amounts of protein were resolved by 12.5% SDS-polyacrylamide gels containing 0.2% gelatin at 4°C. Gels were removed and enzymes renatured in 65 mM Tris buffer, pH 7.4 with 20% glycerol for 3 washes at 10 minutes each. Gels were then incubated in activity buffer (0.1 M sodium phosphate buffer, pH 6.0, 1 mM EDTA, and 2 mM DTT freshly added) for 30 minutes at room temperature. Then this activity buffer was exchanged for fresh activity buffer and incubated for 18–24 hours (overnight) at 37°C. The gels were rinsed twice with deionized water and incubated for one hour in Coomassie stain (10% acetic acid, 25% isopropanol, 4.5% Coomassie Blue) followed by destaining (10% isopropanol and 10% acetic acid). Gels were scanned using an Imagequant 4010 (GE Healthcare). Images were inverted in Adobe Photoshop and densitometry performed using Scion Image (Scion Corporation).

Immunohistochemistry—Localization of cathepsin K protein expression within the aortic wall was determined by immunohistochemistry of aortas. Aortic arches were snap frozen in OCT embedding medium and stored at −80°C until sectioned. Tissue sections (8 μm thick) were obtained using a Leica CM3050 Cryostat and mounted on glass slides. Sections were fixed in acetone, rinsed with PBS, and then blocked in 3% BSA for an hour. Sections were immunolabeled with primary rabbit-anti cathepsin K antibodies (Santa Cruz) at 4°C overnight at a 1:100 dilution in 1% BSA and then probed with tritc anti-rabbit fluorescent secondary antibodies (Santa Cruz) at 37°C for an hour at a 1:100 dilution in PBS in the dark. Negative controls were incubated in 1% BSA overnight and the secondary was added as described previously to rule out non-specific binding. Sections were then mounted using DAPI Pro-long gold antifade reagent and imaged using a Nikon TI-E.

Statistical Analysis

Means between groups were compared using unpaired student t tests with significance at $p < 0.05$.

Results

Arteries from mice expressing HIV proteins exhibit endothelial dysfunction

Isometric relaxation tests on aortic rings exposed to acetylcholine (an endothelial-dependent vasodilator) and sodium nitroprusside (an endothelial-independent vasodilator) were performed to assess endothelial and smooth muscle vaso-regulatory function, respectively. The concentration-relaxation curves of acetylcholine were different between the HIV Tg and wildtype mouse aortic rings, with HIV Tg aortic rings having decreased relaxation (Figure 1A). No differences were observed in the concentration-relaxation curves of sodium nitroprusside in the aortas across groups (Figure 1B). Thus, the difference in total relaxation

(94.84% ± 2.893 and 73% ± 4.780 for WT and HIV Tg respectively, $p < 0.05$, N=10 for WT, N=9 for HIV Tg Figure 1C) is due to endothelial dysfunction.

Arteries from mice expressing HIV proteins exhibit altered arterial biomechanics, including elevated arterial stiffness

Cylindrical biaxial biomechanical testing revealed that the common carotid arteries from the HIV Tg mice have a smaller diameter for a given pressure, with statistically significant differences at pressures between 60 and 100 mm Hg ($p<0.05$, N=9) for the *in vivo* axial stretch ($\lambda=1.7$, Figure 2A) and subphysiological stretch ($\lambda=1.4$, data not shown). No differences were observed in aortic diameters (Figure 2C).

HIV Tg arteries exhibited elevated arterial stiffness (as defined by the Peterson's Modulus), compared to wildtype arteries. Differences were seen at pressures between 20 and 60 mmHg for common carotid arteries at the *in vivo* axial stretch ($\lambda=1.7$; Figure 2B), as well as at subphysiological ($\lambda=1.4$) and superphysiological ($\lambda=1.9$) stretches (data not shown). Similarly, differences were seen in aortas of HIV Tg at pressures of 20 to 40 mm Hg for the *in vivo* axial stretch ($\lambda=1.7$) (Figure 2D), and at subphysiological ($\lambda=1.4$) and superphysiological ($\lambda=1.9$) stretches (data not shown). No differences were observed in the axial force during fixed length pressure-diameter tests over physiologically-relevant loads; differences were observed under very low loads (data not shown). No differences were observed in the *in vivo* axial stretch across groups. There was no difference in the axial force-length behavior of the vessels over physiologically relevant loads; differences were observed at the low stretches and low pressures (data not shown).

Carotid arteries and suprarenal aortas from HIV Tg mice had larger opening angles compared to wildtype arteries (63.7±10.5 vs. 46.2±8.4 for carotid, 139.5±10.4 vs. 83.5±12.5 for aorta, $p<0.05$ N=6, data reported as mean ± SEM, Figure 3). The increased opening angle in the HIV Tg mice indicated there was a greater residual stress in the vessel wall in the unloaded state.

Mice expressing HIV proteins show increased carotid intima-media thickness

HIV Tg mice show increased c-IMT compared to control mice, confirmed by both the histological and two-photon microscopy methods (Figure 4). Microscopy images of the arteries in a loaded state (pressure=100 mmHg and $\lambda=1.7$) revealed an increased medial thickness in the HIV Tg mice for both the suprarenal aorta (31.6 ± 1.7 vs. 17.7 ± 1.3 μm) and carotids (12.3 ± 0.5 vs 24.3 ± 1.4 μm), and the carotids in the HIV Tg mice also had advential thickening (6.3 ± 0.8 vs 12.5 ± 0.7 μm) ($p<0.05$ N=6, Figure 4 B). Note that the value of mean c-IMT measured from fixed tissue was different from that measured with two-photon microscopy as it was in a loaded configuration while the histology measurements were from fixed unloaded tissue.

Collagen Fiber Angles are similar between groups

Fast Fourier transform techniques were used to calculated the average of fiber angle distribution through the wall (figure 5 A); however, the weighted mean fiber angles for the

vessels (a measure of the peak) showed no significant differences in distribution ($p<0.05$, N=6, Figure 5 B).

Aorta from mice expressing HIV proteins have a lower elastin content

Aortas from the HIV Tg mice had less elastin than the wildtype mice ($p<0.05$ N=6, Figure 6); decreased elastin content from the common carotid arteries were not significant ($p=0.21$ N=9). Similarly a non-significant trend of increased collagen in the HIV Tg mice was found for both the aorta and carotids ($p=0.069$ N=6 and $p=0.18$ N=5 respectively). The decrease in elastin content and trend in increased collagen content aligns well with the finding that vessels from HIV Tg have increased arterial stiffening.

Aorta from mice expressing HIV proteins exhibit increased cathepsin K and S activity

Cathepsins K, S, and V are potent elastases. Zymographical analysis of homogenized aortas from HIV-Tg and wildtype mice showed a significant increase in the activity of extracellular matrix bound cathepsin K (75 and 50 kd) and cathepsin S (32 kd). A 6-fold increase in Cathepsin K activity and a 3-fold increase in Cathepsin S activity was observed (N=4 $p<0.05$) (Figure 7 A&B). Cathepsin V was decreased in the HIV Tg aortas as compared to the aortas from wildtype mice (N=3 $p<0.05$). Increased cathepsin activity was confirmed via fluorescent immunohistochemistry on aortic arch sections. There was an increase in cathepsin K visualized throughout the intima-media layer of the HIV Tg aorta as seen in bright red. (Figure 7 C&D). Increased proteolytic activity by cathepsins supports the finding of decreased elastin in the HIV Tg aortas.

Discussion

Mice expressing HIV proteins exhibit endothelial dysfunction and increased intima-media thickness and arterial stiffness

Clinical data clearly show endothelial dysfunction [8, 9, 14, 19, 20], increased arterial stiffness [8, 21, 44–47], and increased c-IMT [8–13] in HIV patients, which have been attributed both to HAART treatment and HIV infection [48]. The present study corroborates these findings in HIV-Tg mice, suggesting that HIV-1 proteins alone, independent of HAART treatment or HIV infection, may play a role in cellular and tissue level remodeling associated with atherosclerosis. Isometric relaxation tests on aortic rings were used to assess endothelial function in this mouse model and found significant endothelial dysfunction in HIV-Tg aorta. Similar relaxation behaviors of the aortic rings to sodium nitroprusside, a nitric oxide (NO) donor, revealed the smooth muscle cells of the arterial wall were still functional and responsive to vasodilative stimuli. However, the decreased relaxation in response to acetylcholine, a vasodilator that acts in an endothelium-dependent manner, is indicative of endothelial dysfunction. Healthy endothelial cells play a role, not only in vasodilation, but also in a number of atheroprotective mechanisms within the vessel wall, and dysfunction of the endothelial layer has been associated with the development of atherosclerosis [49]. Thus, this finding suggests that HIV-1 proteins cause impaired endothelial function and may contribute to the development of atherosclerosis.

Lorenz et al., suggest that HIV-1 and HAART are independent mediators of c-IMT. Their studies found that the intima-media thickness of the carotid bifurcation was 24.8% higher in HIV-1 positive/HAART-naïve patients compared to uninfected controls, but they observed significantly greater intima-media thickness of the carotid bifurcation and the common carotid artery due to HAART treatment in HIV-1 positive subjects, compared to HIV-positive/HAART naïve subjects [50]. Arteries from the HIV-1 Tg mouse exhibited increased intima-media thickness; this finding indicates that HIV-1 proteins alone may play a role in cellular and tissue level remodeling associated with atherosclerosis.

Arterial stiffening is an important clinical marker of cardiovascular disease and a key predictor of future cardiovascular events [51]. Rigorous mechanical tests on aorta and common carotid arteries from the HIV-TG and wild-type mice revealed that arteries were stiffer in HIV-Tg mice, indicating the HIV proteins alone may play a role in increased stiffness. Also, although HIV-associated immune dysfunction is known to play a role in atherosclerotic development [49] and has been associated with arterial stiffness in HIV-infected subjects [45], since this mouse model lacks infected immune cells, it shows that the proteins themselves can mediate the arterial stiffening in this mouse model through mechanisms yet to be determined.

Markers of vascular remodeling consistent with early on-set atherosclerosis

In addition to providing parallel data to support clinical observations in HIV-patient populations and isolating the role of a single mediator (e.g., HIV proteins) on disease progression, animal models allow for measurements that cannot be obtained from human subjects. Biomechanical analysis revealed that, although differences were observed in the circumferential arterial stiffness in HIV-Tg mice, there were few mechanical differences in the axial direction. Also, observed differences in opening angle suggest differences in the local, *in vivo*, mechanical environment (i.e., the local stresses) under physiological loads at different locations across the vessel wall. Such differences in the local mechanical environment may provide insights into local differences in mechanically-mediated biological responses.

Vascular remodeling occurs in part by synthesis, proteolytic degradation, and remodeling of key structural components of the arterial wall (e.g., elastin and collagen) and changes in vascular functional (e.g., endothelial dysfunction), which can lead to changes geometric and biomechanical properties of the artery (e.g., c-IMT, and arterial stiffness, respectively). While the differences in collagen were not statistically significant, aortas from HIV Tg mice had significantly less elastin. Loss of functional elastin is often attributed with arterial stiffening and is common with aging, aneurysm development, and atherosclerosis [52, 53]. Thus, the observed decrease in elastin supports the observed increases in arterial stiffness in HIV-Tg mice.

The cysteine cathepsin family of proteases in humans and mouse models of atherosclerosis are known to play a key role in vascular remodeling [54–56]; cathepsin activity is upregulated in atheroprone regions of the vasculature [57]. Zymography revealed cathepsin K activity in the arterial wall was increased six-fold in the presence of HIV proteins while cathepsin S was increased three-fold. These changes in cathepsin levels (Figure 7) may

occur as the result of impaired nitric oxide production and bioavailability (Figure 1) and/or pro-inflammatory viral proteins, thereby increasing elastolytic activity and degrading elastin in the arterial wall (Figure 6), leading to maladaptive remodeling that increases arterial stiffness (Figure 2), opening angle (Figure 3), and c-IMT (Figure 4).

Potential Mechanisms: Direct affect of HIV proteins on vascular cells

This paper presents observational results that expression of HIV proteins leads to geometric, functional, and biomechanical changes that parallel clinical observations in HIV populations. The mechanisms by which HIV proteins lead to such changes, however, remain unknown. HIV-1 has not been shown to infect vascular endothelial cells *in vivo*; however, it is postulated that in HIV-infected populations endothelial dysfunction may be caused by exposure to circulating infected CD4+ T cells and monocytes as well as viral proteins that have been released into the blood [30–32]. The *tat* protein, which is actively secreted by infected cells, has been found to have a variety of negative effects on the vasculature. Namely, *tat* has decreased the ability of pig coronary arteries to dilate by the inhibiting the expression of nitric oxide synthase (NOS) and thus NO availability [31]. Exposure of endothelial cells to *tat* caused the release monocyte chemoattractant protein-1 (MCP-1), which increases adhesion to the endothelium and transendothelial migration of circulating mononuclear cells into the vascular wall [32]. Numerous other studies have found various other effects of *tat*, *gp120*, *vpu*, and *nef* proteins on endothelial cells including expression of cell adhesion molecules, increased endothelial permeability, cell proliferation, cytokine signaling, apoptosis, and oxidative stress [30]. Therefore, this non-infectious mouse model has a similar phenotype to the altered signaling and function that has been observed in vascular endothelial cells exposed to HIV-1 proteins.

Potential Mechanisms: Secondary effect of other systemic changes

While there are compelling arguments to suggest that the observed vascular changes may be a direct result of HIV-1 proteins on vascular cells, there are also compelling arguments to suggest that these observations are a secondary effect of other systemic changes, such as end-stage organ disease, dyslipidemia, hypertension, and/or inflammation. For example, Kopp et al. reported that the NL4-3Δ *gag/pol* transgenic hemizygous mice develop proteinuria by 4 weeks of age and end-stage renal disease by 14 weeks [33]. Such renal disease and associated hypertension could lead to some of the observed vascular changes reported here.

In summary, while the HIV-Tg mice did not develop atherosclerosis in the time course of this study, they did exhibit several characteristics that are indicative of pre-clinical atherosclerosis. The HIV-Tg mouse model offers the advantage of isolating the effects of the viral proteins not possible clinically. While data from clinical studies have found that HIV-1 positive patients exhibit early markers of atherosclerosis, some discrepancies still exist between studies due the inability to control other cardiovascular risk factors such as age, gender, weight, cholesterol levels, smoking, and hypertension in all patients as well the confounding effects from HAART therapy. This study isolates the *in vivo* effects of the HIV-1 proteins in a mouse model without such confounding factors. Whereas *in vitro* studies have observed some effects such as endothelial dysfunction and monocyte adhesion

[30–32, 58], those *in vitro* models do not allow for the study of clinically observed characteristics such as arterial stiffening and thickening. Not withstanding the numerous differences in mouse models compared to humans disease, these findings support the further use of this animal model to investigate mechanisms involved in the progression of HIV-associated atherosclerosis.

Acknowledgments

We gratefully acknowledge the support from the National Institutes of Health and the International AIDS Society through the Creative and Novel Ideas in HIV Research (CNIHR) Program, the American Heart Association (11GRNT7990055), and the National Science Foundation Graduate Research Fellowship Program (LH).

References

1. USAID. 2008 Report on the global AIDS epidemic. 2008
2. Currier JS, Taylor A, Boyd F, Dezii CM, Kawabata H, Burtcel B, Maa JF, Hodder S. Coronary heart disease in HIV-infected individuals. Journal of Acquired Immune Deficiency Syndromes. 2003 Aug 1.33:506–512. [PubMed: 12869840]
3. Mary-Krause M, Cotte L, Simon A, Partisani M, Costagliola D. Increased risk of myocardial infarction with duration of protease inhibitor therapy in HIV-infected men. AIDS. 2003 Nov 21.17:2479–2486. [PubMed: 14600519]
4. Friis-Moller N, Sabin CA, Weber R, d'Arminio Monforte A, El-Sadr WM, Reiss P, Thiebaut R, Morfeldt L, De Wit S, Pradier C, Calvo G, Law MG, Kirk O, Phillips AN, Lundgren JD. Combination antiretroviral therapy and the risk of myocardial infarction. New England Journal of Medicine. 2003 Nov 20.349:1993–2003. [PubMed: 14627784]
5. Maggi P, Lillo A, Perilli F, Maserati R, Chirianni A. Colour-Doppler ultrasonography of carotid vessels in patients treated with antiretroviral therapy: a comparative study. AIDS. 2004 Apr 30.18:1023–1028. [PubMed: 15096805]
6. Meng Q, Lima JA, Lai H, Vlahov D, Celentano DD, Strathdee SA, Nelson KE, Wu KC, Chen S, Tong W, Lai S. Coronary artery calcification, atherogenic lipid changes, and increased erythrocyte volume in black injection drug users infected with human immunodeficiency virus-1 treated with protease inhibitors. American Heart Journal. 2002 Oct.144:642–648. [PubMed: 12360160]
7. Kaplan RC, Kingsley LA, Sharrett AR, Li X, Lazar J, Tien PC, Mack WJ, Cohen MH, Jacobson L, Gange SJ. Ten-year predicted coronary heart disease risk in HIV-infected men and women. Clinical Infectious Diseases. 2007 Oct 15.45:1074–1081. [PubMed: 17879928]
8. van Vonderen MGA, Hassink EAM, van Agtmael MA, Stehouwer CDA, Danner SA, Reiss P, Smulders Y. Increase in Carotid Artery Intima-Media Thickness and Arterial Stiffness but Improvement in Several Markers of Endothelial Function after Initiation of Antiretroviral Therapy. Journal of Infectious Diseases. 2009 Apr.199:1186–1194. [PubMed: 19275490]
9. Oliviero U, Bonadies G, Apuzzi V, Foggia M, Bosso G, Nappa S, Valvano A, Leonardi E, Borgia G, Castello G, Napoli R, Sacca L. Human immunodeficiency virus per se exerts atherogenic effects. Atherosclerosis. 2009 Jun.204:586–589. [PubMed: 19084229]
10. Hsue PY, Lo JC, Franklin A, Bolger AF, Martin JN, Deeks SG, Waters DD. Progression of atherosclerosis as assessed by carotid intima-media thickness in patients with HIV infection. Circulation. 2004 Apr 6.109:1603–1608. [PubMed: 15023877]
11. Mercie P, Thiebaut R, Aurillac-Lavignolle V, Pellegrin JL, Yvorra-Vives MC, Cipriano C, Neau D, Morlat P, Ragnaud JM, Dupon M, Bonnet F, Lawson-Ayayi S, Malvy D, Roudaut R, Dabis F. Carotid intima-media thickness is slightly increased over time in HIV-1-infected patients. HIV Med. 2005 Nov.6:380–387. [PubMed: 16268819]
12. McComsey GA, O'Riordan M, Hazen SL, El-Bejjani D, Bhatt S, Brennan ML, Storer N, Adell J, Nakamoto DA, Dogra V. Increased carotid intima media thickness and cardiac biomarkers in HIV infected children. AIDS. 2007 May 11.21:921–927. [PubMed: 17457085]

13. Hsue PY, Hunt PW, Schnell A, Kalapus SC, Hoh R, Ganz P, Martin JN, Deeks SG. Role of viral replication, antiretroviral therapy, and immunodeficiency in HIV-associated atherosclerosis. AIDS. 2009 Jun 1.23:1059–1067. [PubMed: 19390417]
14. Bonnet D, Aggoun Y, Szezepanski I, Bellal N, Blanche S. Arterial stiffness and endothelial dysfunction in HIV-infected children. AIDS. 2004 Apr 30.18:1037–1041. [PubMed: 15096807]
15. Sevastianova K, Sutinen J, Westerbacka J, Ristola M, Yki-Jarvinen H. Arterial stiffness in HIV-infected patients receiving highly active antiretroviral therapy. Antivir Ther. 2005; 10:925–935. [PubMed: 16430198]
16. Hsue PY, Hunt PW, Wu Y, Schnell A, Ho JE, Hatano H, Xie Y, Martin JN, Ganz P, Deeks SG. Association of abacavir and impaired endothelial function in treated and suppressed HIV-infected patients. AIDS. 2009 Sep 24.23:2021–2027. [PubMed: 19542863]
17. Blanco JJ, Garcia IS, Cerezo JG, de Rivera JM, Anaya PM, Raya PG, Garcia JG, Lopez JR, Hernandez FJ, Rodriguez JJ. Endothelial function in HIV-infected patients with low or mild cardiovascular risk. Journal of Antimicrobial Chemotherapy. 2006 Jul.58:133–139. [PubMed: 16702174]
18. Grubb JR, Dejam A, Voell J, Blackwelder WC, Sklar PA, Kovacs JA, Cannon RO, Masur H, Gladwin MT. Lopinavir-ritonavir: effects on endothelial cell function in healthy subjects. Journal of Infectious Diseases. 2006 Jun 1.193:1516–1519. [PubMed: 16652279]
19. Torriani FJ, Komarow L, Parker RA, Cotter BR, Currier JS, Dube MP, Fichtenbaum CJ, Gerschenson M, Mitchell CK, Murphy RL, Squires K, Stein JH. Endothelial function in human immunodeficiency virus-infected antiretroviral-naive subjects before and after starting potent antiretroviral therapy: The ACTG (AIDS Clinical Trials Group) Study 5152s. Journal of the American College of Cardiology. 2008 Aug 12.52:569–576. [PubMed: 18687253]
20. Teixeira HN, Mesquita ET, Ribeiro ML, Bazin AR, Mesquita CT, Teixeira MP, Pellegrini Rda C, Nobrega AC. Study of vascular reactivity in HIV patients whether or not receiving protease inhibitor. Arquivos Brasileiros de Cardiologia. 2009 Oct.93:367–373. 360–366. [PubMed: 19936456]
21. van Wijk JP, de Koning EJ, Cabezas MC, Joven J, op't Roodt J, Rabelink TJ, Hoepelman AM. Functional and structural markers of atherosclerosis in human immunodeficiency virus-infected patients. Journal of the American College of Cardiology. 2006; 47:1117–1123. [PubMed: 16545639]
22. Stein JH, Klein MA, Bellehumeur JL, McBride PE, Wiebe DA, Otvos JD, Sosman JM. Use of human immunodeficiency virus-1 protease inhibitors is associated with atherogenic lipoprotein changes and endothelial dysfunction. Circulation. 2001 Jul 17.104:257–262. [PubMed: 11457741]
23. Shankar SS, Dube MP, Gorski JC, Klaunig JE, Steinberg HO. Indinavir impairs endothelial function in healthy HIV-negative men. American Heart Journal. 2005 Nov.150:933. [PubMed: 16290967]
24. Friis-Moller N, Weber R, Reiss P, Thiebaut R, Kirk O, d'Arminio Monforte A, Pradier C, Morfeldt L, Mateu S, Law M, El-Sadr W, De Wit S, Sabin CA, Phillips AN, Lundgren JD. Cardiovascular disease risk factors in HIV patients--association with antiretroviral therapy. Results from the DAD study. AIDS. 2003 May 23.17:1179–1193. [PubMed: 12819520]
25. Grubb J, Dejam A, Voell J, Blackwelder W, Sklar P, Kovacs J, Cannon R, Masur H, Gladwin M. Lopinavir-ritonavir: effects on endothelial cell function in healthy subjects. Journal of Infectious Diseases. 2006 Jul 01.193:1516–1519. [PubMed: 16652279]
26. Choi AI, Vittinghoff E, Deeks SG, Weekley CC, Li Y, Shlipak MG. Cardiovascular risks associated with abacavir and tenofovir exposure in HIV-infected persons. AIDS. 2011 Jun 19.25:1289–1298. [PubMed: 21516027]
27. Worm SW, Sabin C, Weber R, Reiss P, El-Sadr W, Dabis F, De Wit S, Law M, Monforte AD, Friis-Moller N, Kirk O, Fontas E, Weller I, Phillips A, Lundgren J. Risk of myocardial infarction in patients with HIV infection exposed to specific individual antiretroviral drugs from the 3 major drug classes: the data collection on adverse events of anti-HIV drugs (D:A:D) study. The Journal of infectious diseases. 2010 Feb 1.201:318–330. [PubMed: 20039804]
28. Lundgren J, Neuhaus J, Babiker A, Cooper D, Duprez D, El-Sadr W, Emery S, Gordin F, Kowalska J, Phillips A, Prineas R, Reiss P, Sabin C, Tracy R, Weber R, Grund B, Neaton J. Use of

nucleoside reverse transcriptase inhibitors and risk of myocardial infarction in HIV-infected patients. AIDS. 2008 Sep 12.22:F17–F24. [PubMed: 18753925]

29. El-Sadr WM, Lundgren JD, Neaton JD, Gordin F, Abrams D, Arduino RC, Babiker A, Burman W, Clumeck N, Cohen CJ, Cohn D, Cooper D, Darbyshire J, Emery S, Fatkenheuer G, Gazzard B, Grund B, Hoy J, Klingman K, Losso M, Markowitz N, Neuhaus J, Phillips A, Rappoport C. CD4+ count-guided interruption of antiretroviral treatment. New England Journal of Medicine. 2006 Nov 30.355:2283–2296. [PubMed: 17135583]
30. Kline ER, Sutliff RL. The roles of HIV-1 proteins and antiretroviral drug therapy in HIV-1-associated endothelial dysfunction. Journal of Investigative Medicine. 2008 Jun.56:752–769. [PubMed: 18525451]
31. Paladugu R, Fu WP, Conklin BS, Lin PH, Lumsden AB, Yao QZ, Chen CY. HIV Tat protein causes endothelial dysfunction in porcine coronary arteries. Journal of Vascular Surgery. 2003 Sep.38:549–555. [PubMed: 12947275]
32. Park I-W, Wang J-F, Groopman JE. HIV-1 Tat promotes monocyte chemoattractant protein-1 secretion followed by transmigration of monocytes. Blood. 2001 Jan 15.97:352–358. 2001. [PubMed: 11154208]
33. Kopp JB, Klotman ME, Adler SH, Bruggeman LA, Dickie P, Marinos NJ, Eckhaus M, Bryant JL, Notkins AL, Klotman PE. PROGRESSIVE GLOMERULOSCLEROSIS AND ENHANCED RENAL ACCUMULATION OF BASEMENT-MEMBRANE COMPONENTS IN MICE TRANSGENIC FOR HUMAN-IMMUNODEFICIENCY-VIRUS TYPE-1 GENES. Proceedings of the National Academy of Sciences of the United States of America. 1992 Mar.89:1577–1581. [PubMed: 1542649]
34. Sutliff RL, Weber CS, Qian J, Miller ML, Clemens TL, Paul RJ. Vasorelaxant Properties of Parathyroid Hormone-Related Protein in the Mouse: Evidence for Endothelium Involvement Independent of Nitric Oxide Formation. Endocrinology. 1999 May 1.140:2077–2083. 1999. [PubMed: 10218957]
35. Sutliff RL, Dikalov S, Weiss D, Parker J, Raidel S, Racine AK, Russ R, Haase CP, Taylor WR, Lewis W. Nucleoside reverse transcriptase inhibitors impair endothelium-dependent relaxation by increasing superoxide. American Journal of Physiology-Heart and Circulatory Physiology. 2002 Dec.283:H2363–H2370. [PubMed: 12388299]
36. Wan W, Yanagisawa H, Gleason R. Biomechanical and Microstructural Properties of Common Carotid Arteries from Fibulin-5 Null Mice. Annals of Biomedical Engineering. 2010; 38:3605–3617. [PubMed: 20614245]
37. Chuong C, Fung Y. On residual stress in arteries. Journal of Biomechanical Engineering. 1986; 108:189–192. [PubMed: 3079517]
38. Wagenseil JE, Nerurkar NL, Knutsen RH, Okamoto RJ, Li DY, Mecham RP. Effects of elastin haploinsufficiency on the mechanical behavior of mouse arteries. Am J Physiol Heart Circ Physiol. 2005 Sep 1.289:H1209–H1217. 2005. [PubMed: 15863465]
39. Zoumi A, Lu XA, Kassab GS, Tromberg BJ. Imaging coronary artery microstructure using second-harmonic and two-photon fluorescence microscopy. Biophysical Journal. 2004 Oct.87:2778–2786. [PubMed: 15454469]
40. Timmins LH, Wu QF, Yeh AT, Moore JE, Greenwald SE. Structural inhomogeneity and fiber orientation in the inner arterial media. American Journal of Physiology-Heart and Circulatory Physiology. 2010 May.298:H1537–H1545. [PubMed: 20173046]
41. Wan W, Dixon JB, Gleason Rudolph L. Constitutive Modeling of Mouse Carotid Arteries Using Experimentally Measured Microstructural Parameters. Biophysical Journal. 2012; 102:2916–2925. [PubMed: 22735542]
42. Li WA, Barry ZT, Cohen JD, Wilder CL, Deeds RJ, Keegan PM, Platt MO. Detection of femtomole quantities of mature cathepsin K with zymography. Analytical Biochemistry. 2010; 401:91–98. [PubMed: 20206119]
43. Wilder CL, Platt MO. Manipulating substrate and pH in zymography protocols selectively identifies cathepsins K, L, S, and V activity in cells and tissues. In Review. 2011
44. van Vonderen MGA, Smulders YM, Stehouwer CDA, Danner SA, Gundy CM, Vos F, Reiss P, van Agtmael MA. Carotid Intima-Media Thickness and Arterial Stiffness in HIV-Infected Patients:

The Role of HIV, Antiretroviral Therapy, and Lipodystrophy. Jaids-Journal of Acquired Immune Deficiency Syndromes. 2009 Feb.50:153–161.

45. Kaplan RC, Sinclair E, Landay AL, Lurain N, Sharrett AR, Gange SJ, Xue X, Parrinello CM, Hunt P, Deeks SG, Hodis HN. T cell activation predicts carotid artery stiffness among HIV-infected women. Atherosclerosis. 2011 Apr 15.
46. Seaberg EC, Benning L, Sharrett AR, Lazar JM, Hodis HN, Mack WJ, Siedner MJ, Phair JP, Kingsley LA, Kaplan RC. Association between human immunodeficiency virus infection and stiffness of the common carotid artery. Stroke. 2010 Oct.41:2163–2170. [PubMed: 20798374]
47. Sevastianova K, Sutinen J, Westerbacka J, Ristola M, Yki-Jarvinen H. Arterial stiffness in HIV-infected patients receiving highly active antiretroviral therapy. Antivir Ther. 2005; 10:925–935. [PubMed: 16430198]
48. Lorenz M, Stephan C, Harmjanz A, Staszewski S, Buehler A, Bickel M, von Kegler S, Ruhkamp D, Steinmetz H, Sitzer M. Both long-term HIV infection and highly active antiretroviral therapy are independent risk factors for early carotid atherosclerosis. Atherosclerosis. 2008 Mar 01.196:720–726. [PubMed: 17275008]
49. Kádár A, Glasz T. Development of atherosclerosis and plaque biology. Cardiovascular Surgery. 2001; 9:109–121. [PubMed: 11250172]
50. Lorenz MW, Stephan C, Harmjanz A, Staszewski S, Buehler A, Bickel M, von Kegler S, Ruhkamp D, Steinmetz H, Sitzer M. Both long-term HIV infection and highly active antiretroviral therapy are independent risk factors for early carotid atherosclerosis. Atherosclerosis. 2007 Jan 31.
51. Arnet D, Evans G, Riley W. Arterial stiffness: a new cardiovascular risk factor? American Journal of Epidemiology. 1994; 140:669–682. [PubMed: 7942769]
52. Fernandez-Moure JS, Vykoukal D, Davies MG. Biology of aortic aneurysms and dissections. Methodist DeBakey cardiovascular journal. 2011 Jul.7:2–7. [PubMed: 21979117]
53. Lee H-Y, Oh B-H. Aging and arterial stiffness. Circulation journal : official journal of the Japanese Circulation Society. 2010 Nov.74:2257–2262. [PubMed: 20962429]
54. SG Sukhova GK, Simon DI, Chapman HA, Libby P. Expression of the elastolytic cathepsins S and K in human atheroma and regulation of their production in smooth muscle cells. The Journal of Clinical Investigation. 1998; 102:576–583. [PubMed: 9691094]
55. Lutgens E, Lutgens SP, Faber BC, Heeneman S, Gijbels MM, de Winther MP, Frederik P, van der Made I, Daugherty A, Sijbers AM, Fisher A, Long CJ, Saftig P, Black D, Daemen MJ, Cleutjens KB. Disruption of the cathepsin K gene reduces atherosclerosis progression and induces plaque fibrosis but accelerates macrophage foam cell formation. Circulation. 2006 Jan 3.113:98–107. [PubMed: 16365196]
56. Sukhova GK, Zhang Y, Pan JH, Wada Y, Yamamoto T, Naito M, Kodama T, Tsimikas S, Witztum JL, Lu ML, Sakara Y, Chin MT, Libby P, Shi GP. Deficiency of cathepsin S reduces atherosclerosis in LDL receptor-deficient mice. J Clin Invest. 2003; 111:897–906. [PubMed: 12639996]
57. Platt MO, Ankeny RF, Shi GP, Weiss D, Vega JD, Taylor WR, Jo H. Expression of cathepsin K is regulated by shear stress in cultured endothelial cells and is increased in endothelium in human atherosclerosis. American Journal of Physiology-Heart and Circulatory Physiology. 2007 Mar. 292:H1479–H1486. [PubMed: 17098827]
58. Matzen K, Dirkx AEM, oude Egbrink MGA, Speth C, Götte M, Ascherl G, Grimm T, Griffioen AW, Stürzl M. HIV-1 Tat increases the adhesion of monocytes and T-cells to the endothelium in vitro and in vivo: implications for AIDS-associated vasculopathy. Virus Research. 2004; 104:145–155. [PubMed: 15246652]

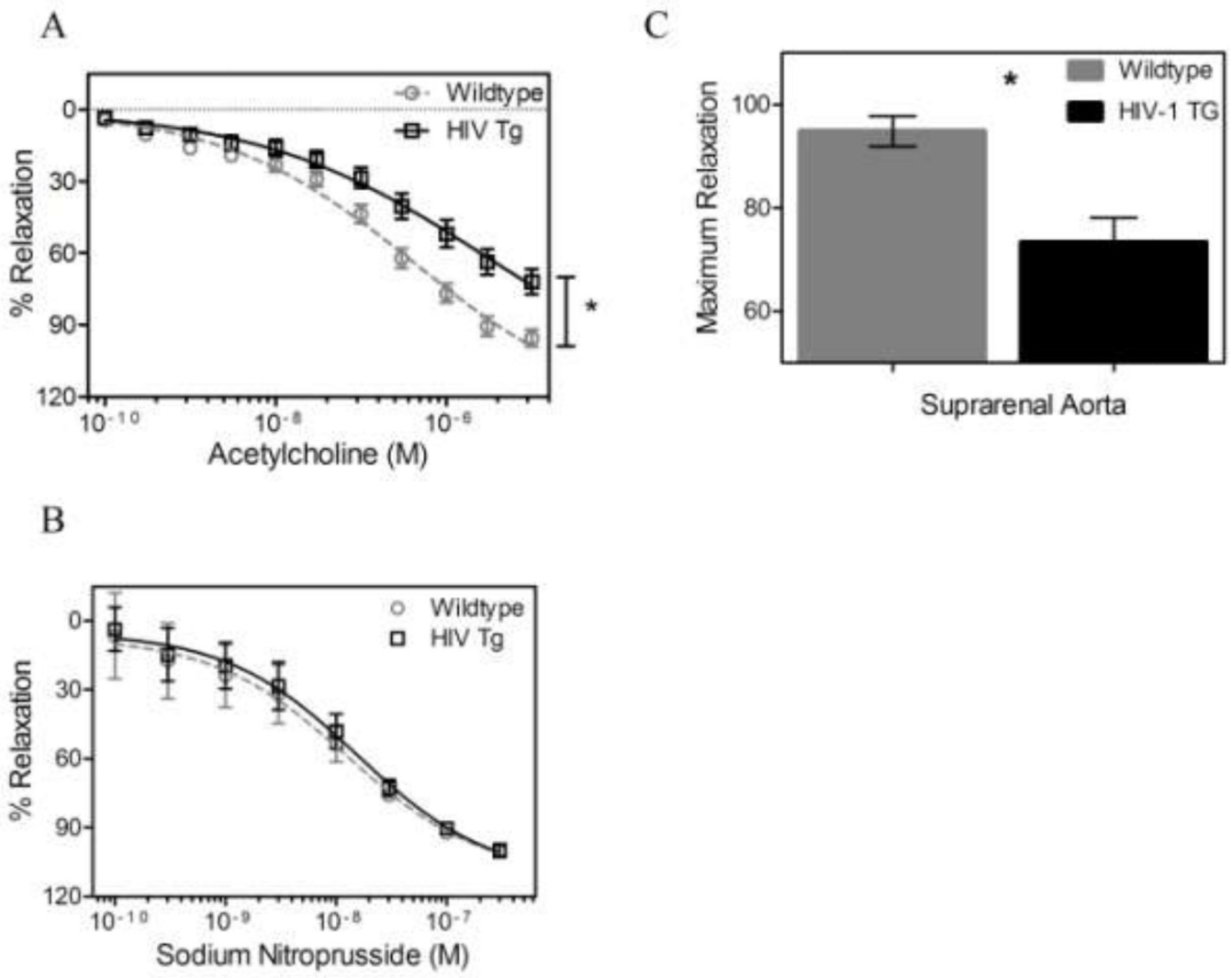

Figure 1. HIV-1 protein expression impairs endothelium-dependent relaxation

Acetylcholine concentration-relaxtion curves for contracted aortic rings (A) for HIV Tg and wildtype mice are different while the sodium nitroprusside curves (B) reveal no differences between groups. Thus, difference in total relaxation (C) (94.84 ± 2.893 and 73 ± 4.780 for WT and HIV Tg respectively) can be attributed to endothelial dysfunction. (* indicates $p < 0.05$, N=10 for WT, N=9 for HIV Tg, and data is mean ± SEM)

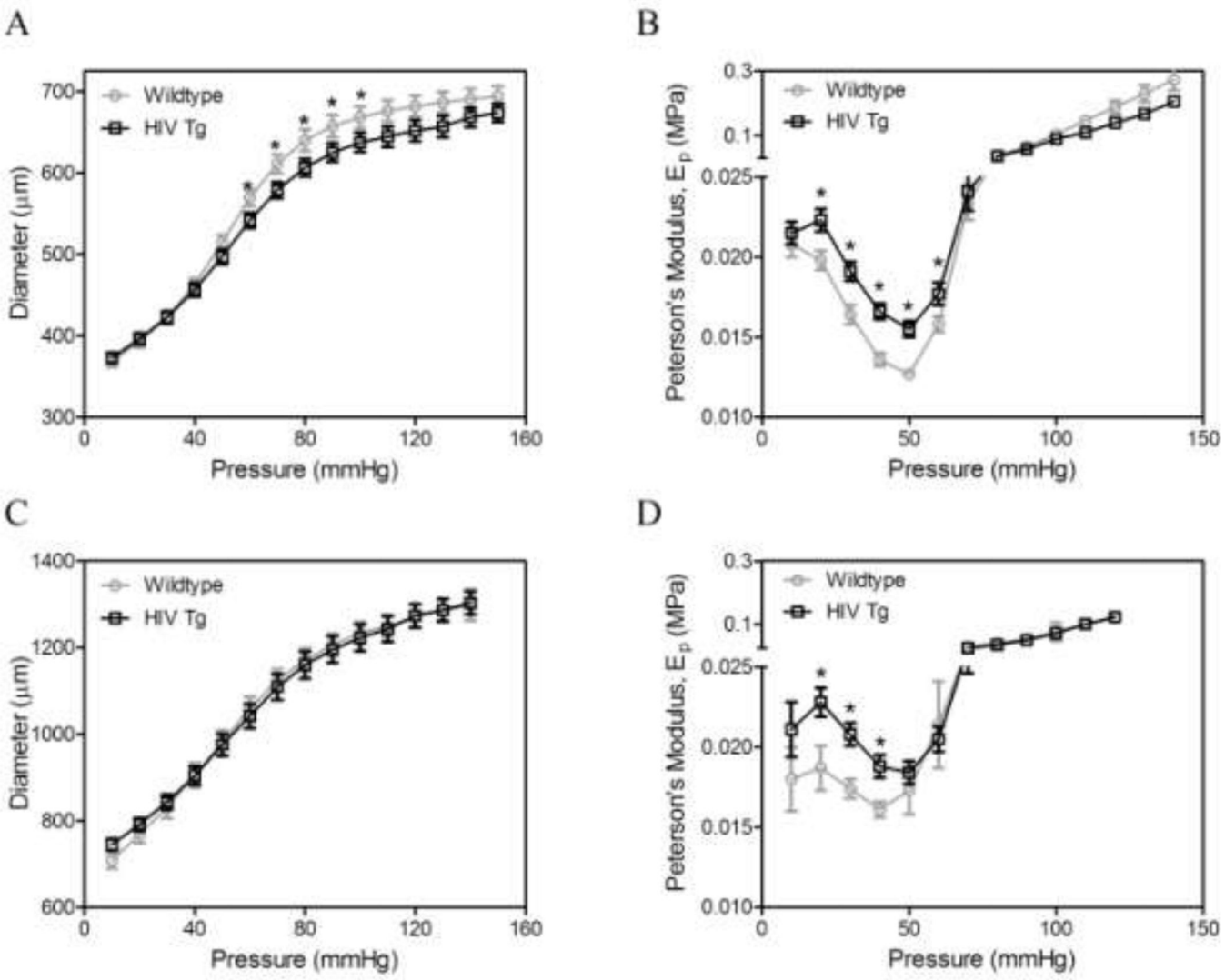

Figure 2. HIV-1 protein expression increases arterial stiffness

Mechanical testing was used to investigate the biomechanics of carotid arteries (A, B) and aortas (C, D). Pressure-diameter mechanical tests (A & C) were performed at a series of fixed stretches. Peterson's modulus, E_p, of the vessels was used to normalize for differences in vessel geometry (B & D, * indicates $p < 0.05$, N=9, and data is mean ± SEM)

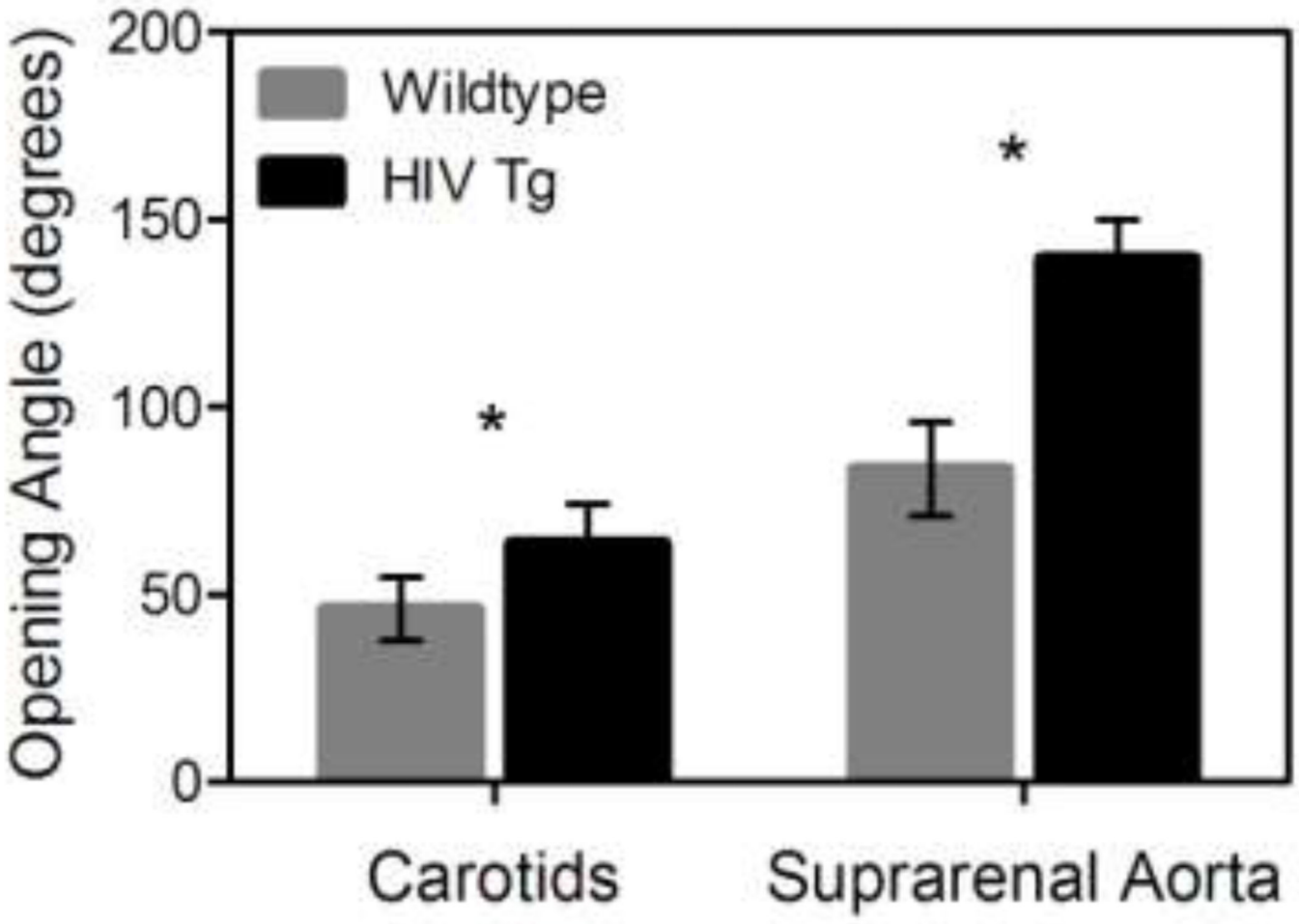

Figure 3. HIV-1 protein expression results in increased opening angle and circumferential residual stress

The residual stress within the vessel wall was calculated by measuring the opening angle of radially cut ring sectors of the arteries. The graph indicates the HIV Tg mice have a greater opening angle and thus more residual stress than the wildtype mice in both the suprarenal aorta and carotid arteries. (* indicates $p < 0.05$ N=6 vessels and data is mean +/− SEM)

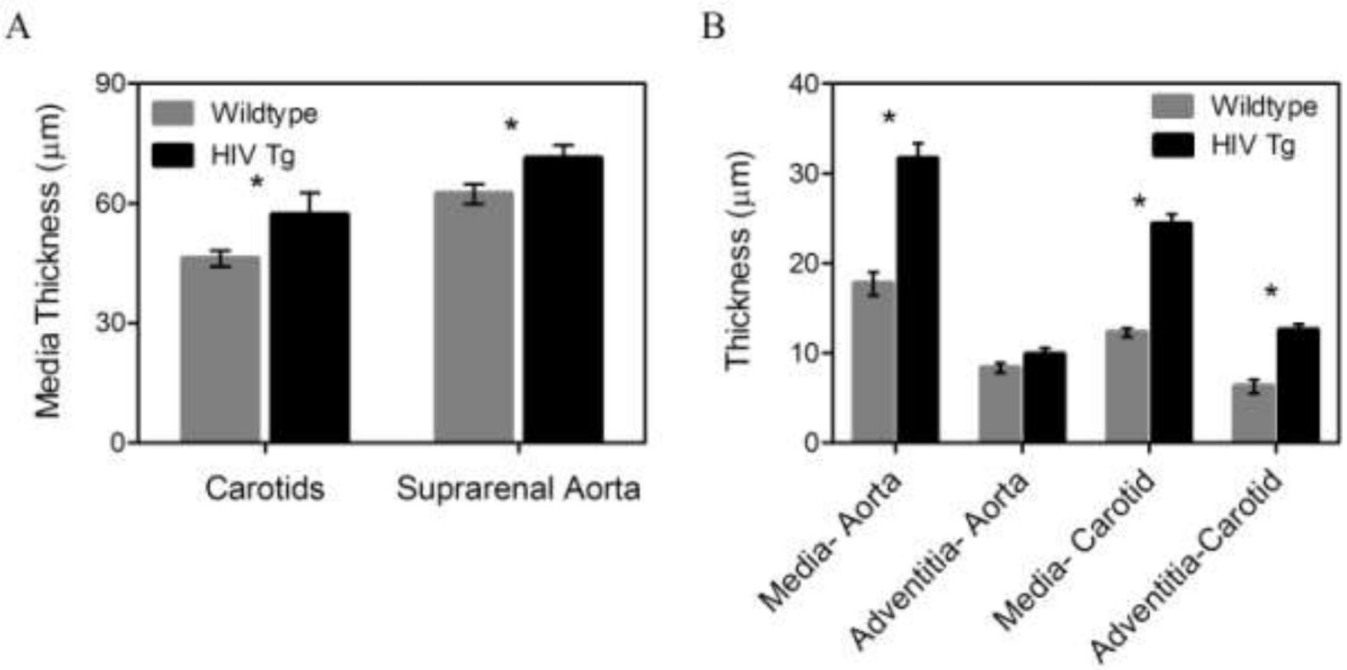

Figure 4. HIV-1 protein expression increases intima-media thickness

Thickness of the arteries was calculated using cross-sectional views from two-photon microscopy stacks of collagen and elastin autofluorescence and histology cross-sections. Panel A shows the intima-media thickness calculated from fixed/frozen histological slides stained with H&E and thickness was calculated using ImageJ. (* indicates $p < 0.05$, N=6, data is mean +/− SEM) Panel B shows the thickness values calculated from cross-sectional views of two-photon microscopy image stacks. The intima-media thickness in both HIV Tg arteries was increased as seen in histology while the adventitia thickness also increased in the HIV Tg carotids only. (* indicates $p < 0.05$. N=6, data is mean +/− SEM)

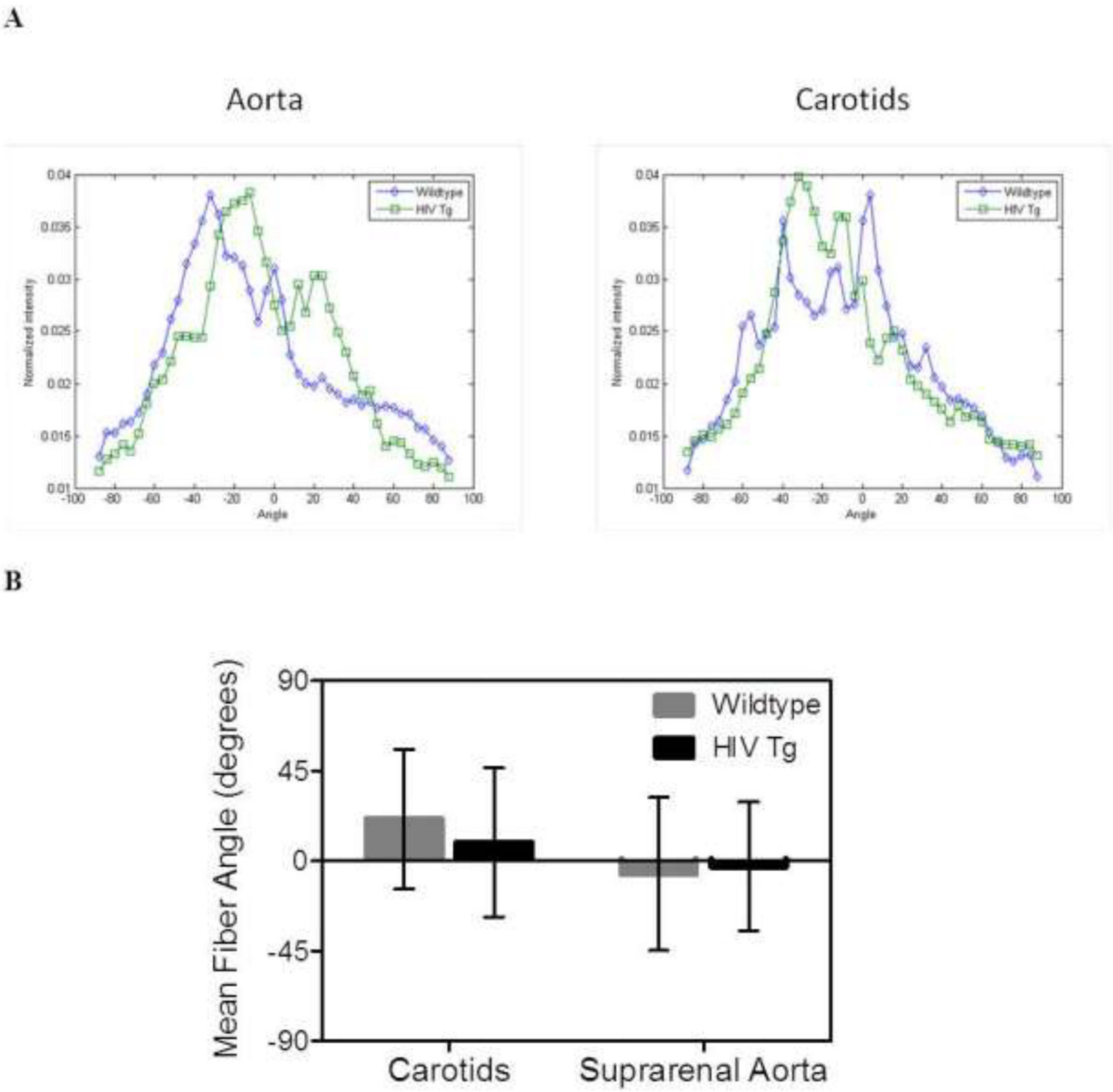

Figure 5. Collagen fiber orientation is not different between groups

The distribution of collagen fibers within the adventitia was determined using fast Fourier transform techniques on images from the two-photon microscopy z-stacks. Panel A shows the average distributions across the wall for the carotids and aortas. Panel B plots the weighted mean fiber angles which show no statistically significant differences are between the HIV Tg and wildtype mice (N=4, $p<0.05$).

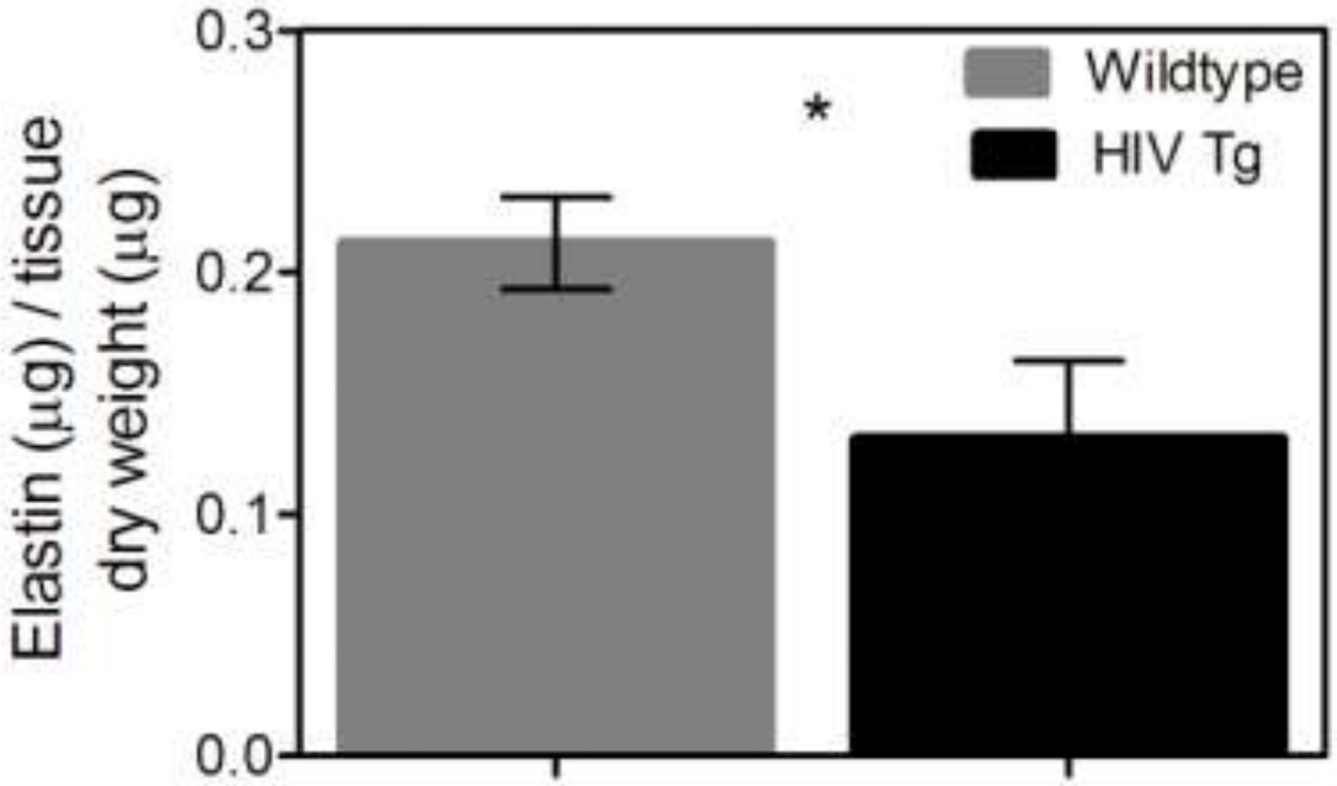

Figure 6. HIV-1 protein expression decreases elastin content

The normalized elastin content of the suprarenal aortas and carotids was determined using the Fastin assay (Biocolor). The HIV Tg aorta had significantly less elastin than the wildtype as shown (HIV Tg = 0.13 µg elastin/µg dry tissue and wildtype= 0.21 µg elastin/µg dry tissue) (* indicate $p<0.05$, N=6, and data is mean +/− SEM). The elastin content of the carotids was not significantly different but had values of 0.32 and 0.37 µg elastin/µg dry tissue for HIV Tg and wildtype respectively ($p=0.21$ N=9). This decrease in elastin aligns with our findings of increased stiffness in the HIV Tg arteries. Collagen content was also assessed using Sirus red staining. The HIV Tg mice had a non-significant trend of more collagen for both the aorta and carotids ($p=0.069$ N=6 and $p=0.18$ N=5 respectively).

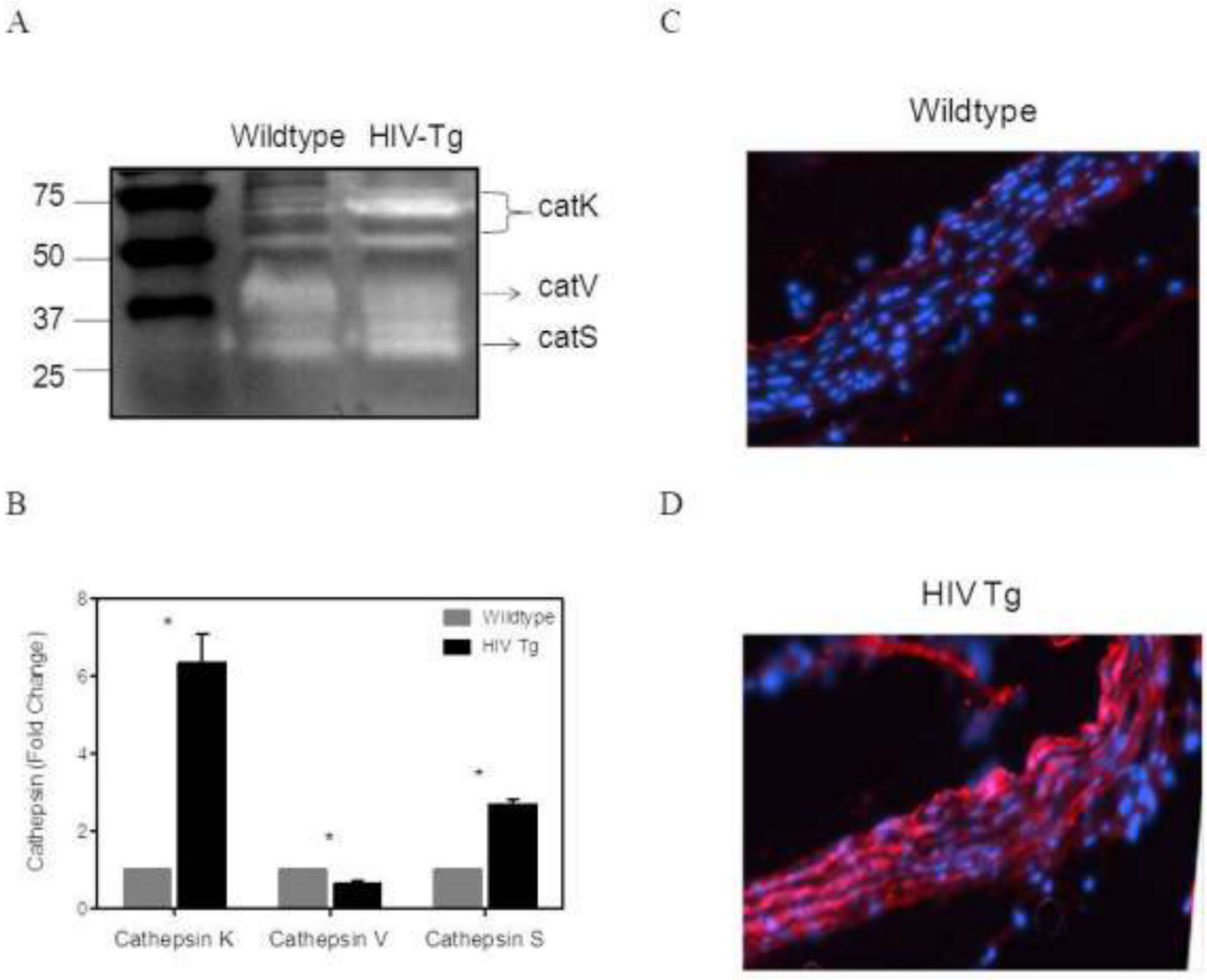

Figure 7. HIV proteins increase cathepsin S and K activity

Cathepsin activity in the arterial wall was determined using zymography and densitometry to quantify the changes. A representative zymography gel is shown in panel A. More pronounced white bands indicate increased cathepsin K and S activity in HIV-Tg mice. The results of the densitometry used to quantify the zymography bands show an increase in cathepsin K and cathepsin S activity in the HIV Tg suprarenal aortas, but a decrease in cathepsin V. (B) (* indicates $p < 0.05$ N=4 (N=3 for cathepsin V) and data is mean +/− SEM) Additionally, immunohistochemistry for Cathepsin K in HIV-Tg and wildtype aortic arches are shown in panel C and D. Cathepsin K, indicated in red, appears to be increased in the HIV-Tg aorta (D).